Available online at www.sciencedirect.com
ScienceDirect
Proceedings of the Combustion Institute 000 (2018) 1–8
Proceedings of the Combustion Institute
www.elsevier.com/locate/proci

Effects of NOx addition on autoignition and detonation development in DME/air under engine-relevant conditions

Peng Dai [a,*], Zheng Chen [b]

[a] *Department of Mechanics and Aerospace Engineering, Southern University of Science and Technology, Shenzhen 518055, China*
[b] *SKLTCS, Department of Mechanics and Engineering Science, College of Engineering, Peking University, Beijing 100871, China*

Received 24 November 2017; accepted 9 June 2018
Available online xxx

Abstract

Exhaust gas recirculation (EGR) technology can be used in internal combustion engines to reduce NOx emission and improve fuel economy. However, it also affects the end-gas autoignition and engine knock since NOx in EGR can promote ignition. In this study, effects of NOx addition on autoignition and detonation development in dimethyl ether (DME)/air mixture under engine-relevant conditions are investigated. Numerical simulation considering both low-temperature and high-temperature chemistry is conducted. First the kinetic effects of NOx addition on the negative temperature coefficient (NTC) regime are assessed and interpreted. It is found that NOx addition greatly promotes both low-temperature and high-temperature ignition stages mainly through increasing OH production. Then the autoignitive reaction front propagation induced by either local NO accumulation or a cold spot within NTC regime with different amounts of NO addition is investigated. For the first time, supersonic autoignition modes including detonation induced by local NO accumulations are identified. This indicates that local accumulation of NOx in end gas might induce super-knock in engines with EGR. A new parameter quantifying the ratio of sound speed to average reaction front propagation speed is introduced to identify the regimes for different autoignition modes. Compared to the traditional counterpart parameter used in previous studies, this new parameter is more suitable since it yields a detonation development regime in a C-shaped curve which is almost unaffected by the initial conditions. The results in this study may provide fundamental insights into knocking mechanism in engines using EGR technology.

Keywords: Autoignition; Detonation development; NOx; DME; Low-temperature chemistry

* Corresponding author.
E-mail address: daip@sustc.edu.cn (P. Dai).

https://doi.org/10.1016/j.proci.2018.06.063
1540-7489

1. Introduction

Recently, downsizing and turbocharging of spark-ignition engines (SIEs) have drawn much attention due to its advantages in fuel economy. However, in highly boosted SIEs knock and super-knock might occur [1,2], which brings great challenge in the development of boosting technologies. It is generally accepted that conventional knock is caused by end gas autoignition while super-knock is closely related to detonation development. Therefore, fundamental understanding of autoignition modes (including detonation development) induced by thermal and/or composition non-uniformity under engine-relevant conditions is needed. On the other hand, exhaust gas recirculation (EGR) technology is increasingly favored to generate leaner and cooler in-cylinder combustion condition which may help to reduce NOx emission and fuel consumption [3–6]. However, EGR can also introduce thermal and/or compositional stratifications within the end gas due to insufficient turbulent mixing. Moreover, NOx in EGR has catalytic effect and it can promote ignition. Therefore, it can affect the autoignition and detonation development in internal combustion engines (ICEs), which has not been comprehensively investigated.

The theory on autoignitive reaction front propagation caused by reactivity non-uniformity was first proposed by Zel'dovich and co-workers [7,8]. Bradley and co-workers [9–12] further developed this theory. They introduced an operational peninsula for detonation development, which can be used to predict engine knock. Specifically, they introduced two non-dimensional parameters, namely the normalized temperature gradient (ξ) and the ratio of acoustic time to excitation time (ε) and found that detonation development occurs within a peninsula in the plot of ξ versus ε [11]. However, only syngas was considered in previous studies. In our recent work [13–15], large hydrocarbon fuels with low-temperature chemistry and negative temperature coefficient (NTC) characteristics were considered. It was found that the reaction-pressure wave interactions become much more complicated in the presence of low-temperature chemistry and that a cold spot can also lead to detonation development when the initial temperature is within NTC regime. Moreover, similar to temperature gradient, concentration gradient can also cause different supersonic autoignition modes including detonation development [16,17].

Previous studies mainly focused on how EGR affects specific heat capacity and mixture dilution (e.g., [3–5]), while there are few studies on the chemical kinetic effects of EGR on autoignition and detonation development process. Foucher and co-workers [18,19] examined ignition enhancement by NO/NO_2 addition in HCCI combustion of n-heptane, iso-octane, toluene and their blends. They found that both the low-temperature and high-temperature ignition stages are promoted when NO is added [18]. Chen et al. [20] found that NO addition suppresses NTC behavior of n-heptane oxidation due to its temperature-dependent impact on ignition. El-Asrag and Ju [6,21] investigated the kinetic effects of NOx addition on autoignition of stratified dimethyl ether (DME)/air mixture in NTC regime. It was found that NO addition dramatically reduces the ignition delay by increasing OH formation. Moreover, two autoignition modes (i.e., spontaneous ignition mode and deflagrative mode) were identified and interpreted. However, to the authors' knowledge, there are no studies focused on how NOx addition affects detonation development under engine-relevant conditions. In engines with EGR strategy, addition of NOx from recirculated exhaust gas may kinetically change the autoignition process of end gas and thereby affect the onset of knock. Therefore, study on how NOx affects autoignition modes and detonation development of large hydrocarbon fuels under engine-relevant conditions is needed. On the other hand, although CO_2, CO and water vapor are present in the mixture in practical engines, their effects on autoignition are much weaker compared to NOx. To simplify the problem, we only considered NOx in this study, and therefore the mixture composition does not fully represent the engine-like conditions.

Based on the above considerations, the objectives of this study are (1) to assess and interpret the kinetic effects of NOx addition (represented by NO and NO_2) on DME/air ignition within NTC regime, and (2) to investigate the autoignition modes induced by NO concentration gradient and temperature gradient in the presence of NO addition, and (3) to examine the effects of NO addition (including local NO accumulation) on detonation development. The detonation development regime for local NO accumulation is obtained for the first time and compared with those for cold spot at different NO addition levels.

2. Numerical model and specifications

As a promising alternative fuel for land transportation, DME has simple chemical structure and typical low-temperature chemistry for NTC behavior which is essentially similar to the main component (e.g., n-heptane, n-decane) of surrogate transportation fuel models. Therefore, DME is chosen as the model fuel in the present study. It is expected that the qualitative trends observed for DME can be extended to larger single-component fuels, at least to n-heptane, which was considered in our previous studies [13,14]. For multi-component fuels, on the other hand, further study is merited since there might be chemical interaction which might change the trends. In order to investigate the autoignition behavior of DME in the presence of NOx, a sub-mechanism of NOx devel-

Please cite this article as: P. Dai, Z. Chen, Effects of NOx addition on autoignition and detonation development in DME/air under engine-relevant conditions, Proceedings of the Combustion Institute (2018), https://doi.org/10.1016/j.proci.2018.06.063

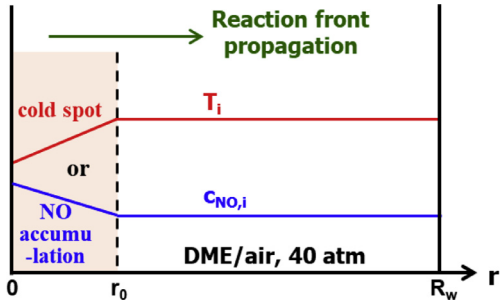

Fig. 1. Schematic of cold spot or NO-accumulation spot for autoignition in DME/air with NO addition in a spherical chamber with the radius of R_W.

oped by Zhao et al. [22] is combined with the recent DME mechanism (Mech_56.54) developed by Burke et al. [23]. This original DME mechanism consists of 113 species and 710 reactions and has pressure-dependent treatment for low-temperature reactions. It was demonstrated to be able to accurately predict ignition (including NTC behavior) of DME/air mixtures at a broad range of temperatures and pressures [23–25]. After including 16 additional species (N, NH, NH_2, NH_3, NO, NO_2, NO_3, HNO, H_2NO, HONO, HNO_2, NNH, N_2H_2, N_2H_3, N_2H_4 and N_2O) accounting for NOx reactions, the combined mechanism has 129 species and 868 reactions. In the Supplemental Material, the combined mechanism is validated against the original DME mechanism [23] for DME/air ignition without NOx addition and against the shock tube experimental data from Ye et al. [26] with different levels of NO_2 addition into DME/O_2/Ar mixture. It is observed that the present combined mechanism has the same performance as the original DME mechanism [23] in terms of predicting ignition of DME/air. Furthermore, good agreement is achieved between numerical prediction and experimental measurement in a broad range of equivalence ratio (0.5–2.0), temperature (1000–1500 K), pressure (4 and 10 atm) and NO_2 concentration (0–17,000 ppm). Therefore, the combined mechanism can be used to study the ignition of DME/air/NOx.

The transient autoignition process is initiated by either NO concentration gradient or temperature gradient (a cold spot) at the center of an adiabatic, closed, spherical chamber. To isolate and identify the effects of concentration/temperature gradient on autoignition, 1D simulation without turbulence was conducted. In fact, turbulence might have great impact on the autoignition process when the characteristic time scales for different processes are comparable. Therefore, further investigation is needed to reveal the turbulent effects on the autoignition behavior observed in this study. As shown in Fig. 1, two types of initial condition for stoichiometric DME/air mixture are considered. The first one is local NO accumulation with uniform initial temperature

$$c_{NO,i}(r) = \begin{cases} c_0 + (r - r_0)(dc_{NO}/dr)_i & (r \le r_0) \\ c_0 (r_0 < r \le R_w) \end{cases}, \quad T_i = T_{i,0} = 940\text{K} \tag{1}$$

and the second one is a cold spot with uniform NO concentration

$$T_i(r) = \begin{cases} T_{i,0} + (r - r_0)(dT/dr)_i & (r \le r_0) \\ T_{i,0} = 975\text{K} & (r_0 < r \le R_w) \end{cases}, \quad c_{NO,i} = c_0 \tag{2}$$

where T_i and $c_{NO,i}$ are respectively initial temperature and NO molar faction, r is radial spatial coordinate, r_0 is the radius of NO-accumulation/cold spot which varies from 3 to 8 mm, $R_W = 4$ cm is the radius of the spherical chamber, $(dc_{NO}/dr)_i$ and $(dT/dr)_i$ are the specified NO concentration gradient and temperature gradient, respectively. It is noted that for these two initial conditions, linear distribution is assumed for NO concentration or temperature within $0 \le r \le r_0$. The mixture is initially static ($u_0 = 0$ m/s) at elevated pressure of $P_0 = 40$ atm. Non-penetrative (e.g., $\partial Y_{NO}/\partial r = 0$, where Y_{NO} is NO mass fraction), adiabatic, reflective boundary conditions are adopted at both boundaries (i.e., $r = 0$ and $r = R_W$).

The autoignition process is simulated using the in-house A-SURF code [27] which solves the conservation equations of 1D, compressible, multi-component, reactive flow using the finite volume method. The mixture-averaged model is used for the species diffusion velocity and thermal diffusion due to temperature gradient is also considered. A dynamically adaptive mesh refinement algorithm is used to efficiently and accurately resolve the propagating reaction front, pressure wave and detonation. The finest mesh size covering them is 3.125 μm and the corresponding time step is 0.625 ns. Grid convergence is achieved as shown in [13–15]. The details on governing equations, numerical scheme and code validation for A-SURF can be found in Refs. [13–15,27] and thereby are not repeated here.

3. Results and discussion

In order to assess the kinetic effect of NOx addition on DME/air ignition, we first studied the 0D constant-volume homogeneous ignition process in stoichiometric DME/air with different amounts of NO and NO_2 addition. Figure 2 shows the results for the initial temperature of $T_0 = 940$ K and pressure of $P_0 = 40$ atm within NTC regime. Figure 2(a) plots the ignition delay times of the first-stage, second-stage and global ignition (i.e., τ_1, τ_2 and τ) as a function of NOx molar fraction in the whole mixture. The first-stage ignition delay is defined as the time when first peak of the heat release rate appears; and the global ignition delay corresponds to

Please cite this article as: P. Dai, Z. Chen, Effects of NOx addition on autoignition and detonation development in DME/air under engine-relevant conditions, Proceedings of the Combustion Institute (2018), https://doi.org/10.1016/j.proci.2018.06.063

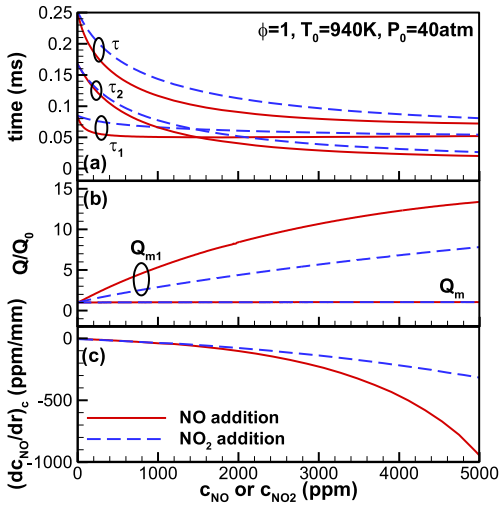

Fig. 2. Effects of NO and NO_2 addition on (a) the first-stage, second-stage and global ignition delay times (i.e., τ_1, τ_2 and τ) in constant-volume homogeneous ignition, (b) the maximum heat release rates at the first-stage ignition (Q_{m1}) and second-stage ignition (Q_m) normalized by their values without NOx addition, and (c) critical NO and NO_2 concentration gradients. The mixture is stoichiometric DME/air initially at $T_0 = 940$ K and $P_0 = 40$ atm.

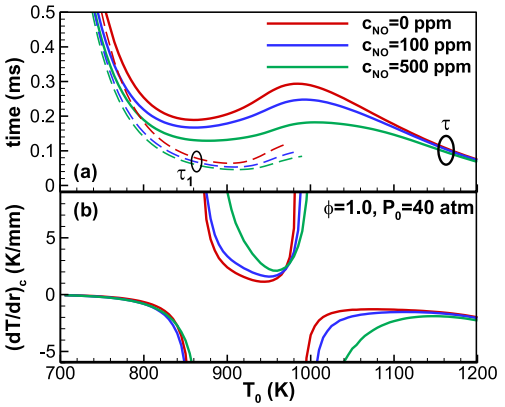

Fig. 3. Effects of NO addition on (a) the first-stage and global ignition delay times (i.e., τ_1 and τ) and (b) critical temperature gradient. The mixture is stoichiometric DME/air at $P_0 = 40$ atm.

the second peak of the heat release rate, the second-stage ignition delay time is equal to their difference (i.e., $\tau_2 = \tau\text{-}\tau_1$). It is seen that both NO and NO_2 addition can greatly reduce the first-stage, second-stage and thereby global ignition delay times. This indicates that similar to a hot/cold spot, local NOx accumulation can induce autoignitive front propagation. Besides, it is observed that the ignition promoting effects gradually decrease with the increase of NOx concentration: at higher concentration such as $c_{NO} \geq 1000$ ppm or $c_{NO2} \geq 2000$ ppm, a further increase of NOx addition has little influence on the ignition delay time. Figure 2(b) shows the maximum heat release rate respectively at the first-stage and global ignition delay times, which are normalized by the values without NOx addition. It is found that NO and NO_2 addition significantly increase the heat release rate at the first-stage low-temperature ignition while having no influence on that at high-temperature ignition. Since the ignition enhancement by NO is much greater than that of NO_2 as shown in Figs. 2(a) and (b), only NO addition is considered in the following discussion.

The effects of NO addition on the NTC behavior of stoichiometric DME/air mixture are shown in Fig. 3(a). Similar results are obtained for rich and lean cases as well as those for NO_2 addition, which are presented in the Supplemental Material. Figure 3(a) shows that although NO addition reduces both the first-stage and global ignition delay times, it does not qualitatively change the NTC behavior. Therefore, a cold spot [13,15] can still induce autoignitive front propagation in NTC regime even with NOx addition.

The kinetic effect of NO addition on DME/air ignition is examined via reaction flux analysis and the key elementary reactions as well as species are identified. The details are shown in the Supplemental Material. For the first ignition stage, it is found that NO addition does not qualitatively change the original reaction pathway of low-temperature chemistry. Instead, most of the NO consumption is through the reaction HO_2+NO=NO_2+OH (R725) which greatly promotes OH production and thereby leads to a faster development of radical pool (OH, H, HO_2, CH_3, etc.). Consequently, the H-abstraction reactions of DME, especially those by OH and H, are significantly enhanced and the key species including methoxymethyl (CH_3OCH_2, denoted as R), methoxymethyl-peroxy ($CH_3OCH_2O_2$, denoted as RO_2) and hydroperoxy-methoxymethyl ($CH_2OCH_2O_2H$, denoted as R'OOH) grow more quickly to higher concentration, leading to a significant promotion of low-temperature chemistry. As a result, the first-stage ignition delay time (τ_1) is reduced and its corresponding heat release rate is increased by NO addition, as shown in Fig. 2. For the second ignition stage, reactions NO_2+CH_3=NO+CH_3O (R729) and NO_2+H=NO+OH (R724) (also produces OH by itself) make the main contribution to the reproduction of NO which further reacts with HO_2 to produce OH via R725. Therefore, with NO addition, the abundance of radical pool and higher temperature after the first ignition stage lead to the reduction of the second-stage ignition delay time (τ_2) as well as the global ignition delay time ($\tau = \tau_1 + \tau_2$).

Please cite this article as: P. Dai, Z. Chen, Effects of NOx addition on autoignition and detonation development in DME/air under engine-relevant conditions, Proceedings of the Combustion Institute (2018), https://doi.org/10.1016/j.proci.2018.06.063

The kinetic effect of NOx addition on DME/air ignition implies that autoignitive front propagation may be induced by either local NOx accumulation or a cold spot in NTC regime with a certain amount of NOx addition. According to the theory of Zel'dovich [8], the autoignitive front propagation speed (u_a) equals to the sound speed, a, at critical temperature gradient given by [9,13]:

$$(dT/dr)_c = (a(d\tau/dT_0))^{-1} \tag{3}$$

Similarly, a critical NO concentration gradient can be defined as:

$$(dc_{NO}/dr)_c = (a(d\tau/dc_{NO}))^{-1} \tag{4}$$

where $d\tau/dT_0$ and $d\tau/dc_{\mathrm{NO}}$ are obtained from simulation of 0D homogeneous ignition (see Figs. 2a and 3a). The critical NO concentration gradient and critical temperature gradient are shown in Figs. 2(c) and 3(b), respectively. The normalized gradient is therefore defined as [9]:

$$\xi = \frac{a}{u_a} = \begin{cases} (dT/dr)_i/(dT/dr)_{c,r_0/2} \\ \quad \text{(cold spot)} \\ (dc_{NO}/dr)_i/(dc_{NO}/dr)_{c,r_0/2} \\ \quad \text{(NO} - \text{accumulation spot)} \end{cases} \tag{5}$$

where the subscript $r_0/2$ denotes that the values of critical gradient are evaluated at the middle of the cold/NO-accumulation spot. Since the initial NO concentration or temperature is assumed to be linearly distributed within $0 \le r \le r_0$, parameters at the middle point (i.e., $r = r_0/2$) are the best choice to represent the average condition within the NO-accumulation or cold spot. Similar treatment was also used in previous studies (e.g., [9,14]).

However, theoretical value, u_a, based on ξ may differ from the actual transient reaction front propagation speed, S, since the transient evolution of NO concentration or temperature gradient is not considered in theory [13]. In order to better quantify the relation between reaction front propagation and autoignition mode, we introduce the following normalized parameter, ξ_a,

$$\xi_a = a_{r_0/2}/S_{AVG} \tag{6}$$

where $a_{r0/2}$ and S_{AVG} are respectively the sound speed at $r = r_0/2$ and average speed of reaction front propagation within cold/NO-accumulation spot (i.e., $0 \le r \le r_0$) calculated from 1D simulation. Since ξ_a is based on the actual reaction front propagation speed, it is expected to be better than ξ in terms of describing different autoignition modes.

The 1D auoignition process induced by local NO accumulation is first investigated (i.e., the initial condition is given in Eq. (1)). The initial temperature is uniformly distributed as $T_i = T_{i,0} = 940$ K and it is within the NTC regime. It is found that with the increase of initial NO concentration gradient (i.e. decrease of autoignitive reaction front propagation speed) at specified NO addition level and NO-accumulation spot size, three autoignition modes sequentially appear, namely (I) supersonic reaction front propagation, (II) detonation development, and (III) subsonic reaction front propagation.

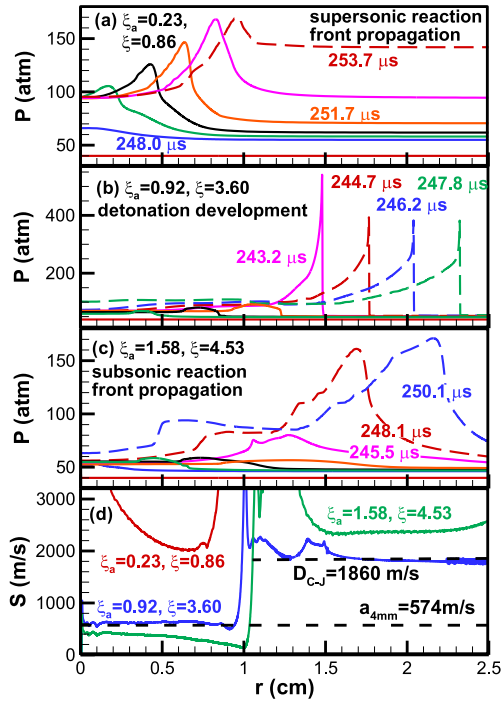

Fig. 4. Temporal evolution of pressure distributions during autoignitive front propagation in stoichiometric DME/air with NO-accumulation spot for (a) $\xi_a = 0.23$, (b) $\xi_a = 0.92$ and (c) $\xi_a = 1.58$ at $T_i = 940$ K and $P_0 = 40$ atm. Figure 4(d) shows the corresponding transient autoignitive reaction front propagation speed for the above three cases. The radius of NO-accumulation spot is $r_0 = 8$ mm and the NO concentration outside the spot is $c_0 = 0$ ppm (i.e., without NO presence outside the spot). The time marked in Fig. 4(a)–(c) indicates the corresponding moment of different curves. The horizontal dashed lines in Fig. 4(d) indicate the C-J detonation wave speed, $D_{C\text{-}J}$, and local sound speed at $r = r_0/2 = 4$ mm, respectively.

Figure 4 shows typical examples of those three modes by plotting the temporal evolution of pressure distributions and corresponding reaction front propagation speed (the evolution of temperature distributions is shown in the Supplemental Material). Figure 4(d) demonstrates that compared to ξ, ξ_a is better to quantify the ratio between transient reaction front propagation speed and local sound speed. Specifically, the autoignitive reaction front propagates around sound speed within NO-accumulation spot when ξ_a approaches unity (i.e., $\xi_a = 0.92$). This leads to a strong coupling and mutual reinforcement between chemical reaction and pressure wave, and thereby detonation develop-

Please cite this article as: P. Dai, Z. Chen, Effects of NOx addition on autoignition and detonation development in DME/air under engine-relevant conditions, Proceedings of the Combustion Institute (2018), https://doi.org/10.1016/j.proci.2018.06.063

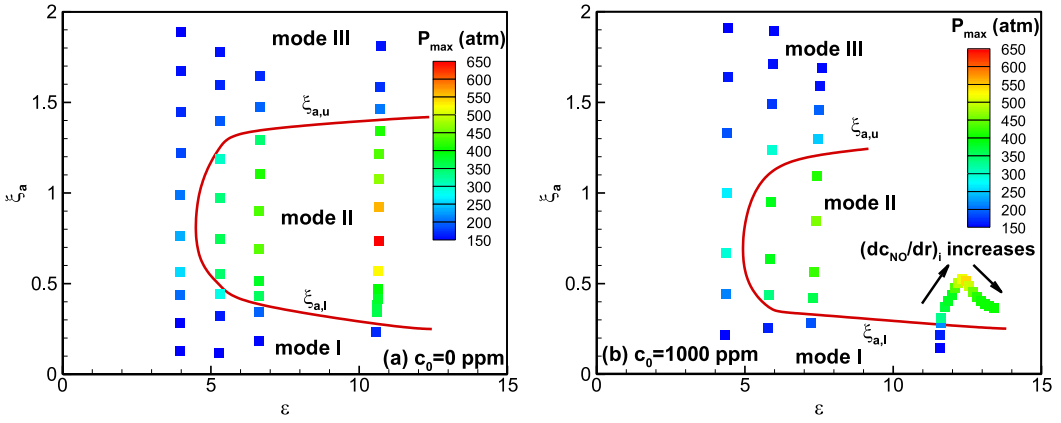

Fig. 5. Autoignition modes induced by NO concentration gradient in stoichiometric DME/air at $T_i = 940$ K and $P_0 = 40$ atm with (a) $c_0 = 0$ ppm and (b) $c_0 = 1000$ ppm. The three modes are (I) supersonic reaction front propagation, (II) detonation development, and (III) subsonic reaction front propagation. The maximum local pressure of each autoignition case is indicated by the color scale.

ment therein. As shown in Fig. 4(b), the peak pressure at $\xi_a = 0.92$ is around 540 atm due to the overdriven detonation and then it stabilizes around 380 atm at a propagation speed close to C-J detonation speed, $D_{C\text{-}J} = 1860$ m/s (see Fig. 4d). On the other hand, supersonic and subsonic reaction front propagation modes are identified at lower and higher values of ξ_a, respectively, with the maximum pressure close to the equilibrium value of $P_e = 142$ atm. For the subsonic reaction front propagation mode shown in Fig. 4(c), global autoignition eventually occurs in the unburned gas and then the autoignition front propagates at a supersonic speed around 2400 m/s, with a peak pressure much higher than the previous subsonic front within the spot (lower than 60 atm). The above results indicate that similar to hot spot outside NTC regime and cold spot within NTC regime [13], local NO accumulation can also induce supersonic autoignition and detonation modes. Therefore, local accumulation of NOx in end gas might induce super-knock in engines with EGR strategy.

Simulations for different NO concentration gradients, different NO-accumulation spot sizes and different NO addition levels are conducted to get detonation development regimes in the plot of ξ_a-ε or ξ-ε. As proposed by Bradley and coworkers [9], ε is defined as the ratio of acoustic time (r_0/a) to excitation time τ_e (the time interval between 5% and maximum heat release rate), i.e., $\varepsilon = r_0/(a\tau_e)$, where a and τ_e are evaluated at $r = r_0/2$. It can be varied by changing the spot size, r_0. In addition, when ξ or ξ_a is changed, ε will also be slightly changed due to the minor change of a and τ_e at $r = r_0/2$.

Figures 5(a) and (b) show the autoignition modes and maximum pressure for cases without NO outside the spot (i.e., $c_0 = 0$ ppm) and with high NO concentration (i.e., $c_0 = 1000$ ppm), respectively. The results for moderate NO addition (i.e., $c_0 = 100$ and 500 ppm) and those in the plot of ξ-ε are shown in the Supplemental Material. A detonation development regime is identified within a C-shaped curve, while the supersonic/subsonic reaction front propagation mode appears below/above its lower/upper branch $\xi_a < \xi_{a,l}$ / $\xi_a > \xi_{a,u}$. For modes I and III, the reaction front propagation speed differs greatly from sound speed, leading to the failure of coherent chemical-acoustic coupling and detonation development. As expected, Fig. 5 also shows that the maximum pressure within the detonation regime is much higher than that of the other two autoignition modes.

Besides, it is found that for large spot size with high NO concentration ($r_0 = 8$ mm and $c_0 = 1000$ ppm as shown in Fig. 5b), ξ_a and ξ do not increase monotonously with NO concentration gradient, $(dc_{NO}/dr)_i$. This is due to the fact that the critical gradient $(dc_{NO}/dr)_c$ increases faster than $(dc_{NO}/dr)_i$ when NO concentration increases within the spot (see Fig. 2c), which reduces the ratio between sound speed and reaction front propagation speed (see Eq. 5). Consequently, ξ_a and ξ first increase and then decrease with the increase of $(dc_{NO}/dr)_i$. This leads to the failure in identifying the upper boundary of detonation regime (i.e., $\xi_{a,u}$) as shown in Fig. 5(b). In such cases, detonation instead of subsonic reaction front propagation mode is triggered even at very high values of $(dc_{NO}/dr)_i$.

The autoignitive reaction front propagation induced by a cold spot within NTC regime at different levels of NO addition (i.e., the initial condition is given in Eq. 2) is also investigated. Similarly, three autoignition modes are also identified and so is a C-shaped detonation regime. The results for cold spot cases without and with moderate NO addition

Please cite this article as: P. Dai, Z. Chen, Effects of NOx addition on autoignition and detonation development in DME/air under engine-relevant conditions, Proceedings of the Combustion Institute (2018), https://doi.org/10.1016/j.proci.2018.06.063

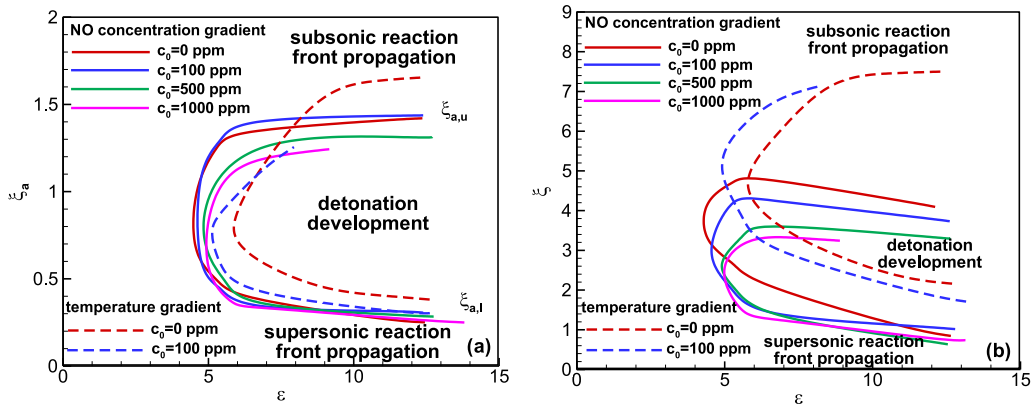

Fig. 6. Regimes of three autoignition modes induced by NO concentration gradient (solid lines) and temperature gradient (dashed lines) for stoichiometric DME/air at $P_0 = 40$ atm in the plots of (a) ξ_a-ε and (b) ξ-ε.

(i.e., $c_{NO} = 0$ and 100 ppm without NO concentration gradient) are shown in the Supplemental Material.

Figure 6 summarizes the detonation regime induced by NO concentration gradient and temperature gradient (cold spot) in the plots of ξ_a-ε and ξ-ε. It is observed in Fig. 6(a) that the C-shaped curves bounding the detonation development regime at different NO addition levels are close to each other, especially for those due to NO concentration gradient. Specifically, the detonation regime with NO concentration gradient is bounded by the upper limit around $\xi_a = 1.3$ and the lower limit around $\xi_a = 0.3$. This demonstrates the advantage of using the parameters ξ_a instead of ξ in the prediction of detonation development regime. Moreover, since ξ_a directly evaluates the ratio of sound speed to transient reaction front propagation speed within the spot, Fig. 6(a) further demonstrates the dominating role of the chemical-acoustic interaction in the onset of different autoignition modes, especially detonation mode (for which strong coupling and mutual reinforcement between chemical reaction and pressure wave occur).

However, Fig. 6(b) shows that the detonation regimes in ξ-ε diagram strongly depend on NO addition levels and spot types. Moreover, the upper limit of detonation regime (ξ_u) with NO concentration gradient decreases monotonously with ε, which is just in the opposite trend to that with temperature gradient including both cold and hot spots (also see Refs. [13,15]). Therefore, the parameter ξ is less effective in terms of predicting detonation development and illuminating the corresponding mechanism in the presence of NO addition, although it can be straightforwardly evaluated from homogeneous ignition delay.

Though detonation development regime can be adequately quantified in the plot of ξ_a-ε, the evaluation of ξ_a requires 1D simulation at least for the period in which reaction front propagates within the NO-accumulation/cold spot. Since ξ can be easily obtained from 0D simulation of homogeneous ignition, it will be useful to know the relationship between ξ_a and ξ.

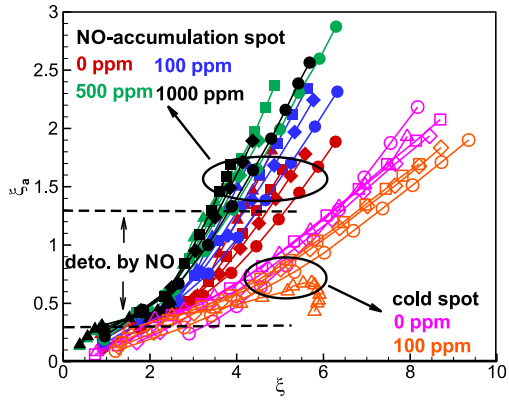

Fig. 7. ξ_a as a function of ξ with NO-accumulation spot (solid symbols) and cold spot (hollow symbols) in stoichiometric DME/air with different amounts of NO addition (represented by six different colors for $c_0 = 0$, 100, 500, 1000 ppm) and $P_0 = 40$ atm. Each curve represents a specified spot radius (i.e., circle, diamond, square and delta symbols respectively represent $r_0 = 3$, 4, 5, 8 mm for all NO-accumulation spots and cold spot with $c_0 = 100$ ppm, and $r_0 = 3$, 5, 6.5, 8 mm for cold spot with $c_0 = 0$ ppm). The upper and lower limits of detonation regime with NO-accumulation spot (i.e., around $\xi_a = 1.3$ and 0.3) are marked by horizontal dashed lines.

Figure 7 compares ξ_a with ξ for all cases considered in this study. With the increase of NO concentration gradient or temperature gradient, ξ_a increases monotonously with ξ. For the same spot type, ξ_a-ξ curves are close to each other with nearly the same slope. However, the discrepancies among

Please cite this article as: P. Dai, Z. Chen, Effects of NOx addition on autoignition and detonation development in DME/air under engine-relevant conditions, Proceedings of the Combustion Institute (2018), https://doi.org/10.1016/j.proci.2018.06.063

them indicate the influence of NO addition level, spot type and spot size. For example, the ξ_a-ξ curve for NO-accumulation spot at given NO addition level is found to shift towards left as the spot radius increases. As a result, the upper bound of C-shaped detonation regime in the plot of ξ-ε decreases with ε for NO-accumulation spot (see Fig. 6b) since $\xi_{a,u}$ keeps almost constant around $\xi_a = 1.3$. Therefore, the effect of initial condition including spot type and size, NO addition level and initial temperature [15] on the relation between ξ_a and ξ merits further investigation for better prediction of detonation development regime.

4. Conclusions

Numerical simulations considering detailed chemistry are conducted to examine the effects of NOx addition on 0D and 1D autoignition in DME/air mixture. For 0D homogenous ignition, NOx addition can significantly reduce the first-stage, second-stage and global ignition delay times, and increase the heat release rate during the first-stage ignition. The ignition enhancement by NO addition is mainly due to the increase in OH production through reactions HO_2+NO=NO_2+OH, NO_2+CH_3=NO+CH_3O and NO_2+H=NO+OH. The 1D transient autoignitive reaction front propagation induced by NO-accumulation and cold spots is systematically investigated for stoichiometric DME/air mixture within NTC regime. Similar to temperature gradient, NO concentration gradient can also induce three typical autoignition modes: (I) supersonic reaction front propagation, (II) detonation development, and (III) subsonic reaction front propagation. This indicates that local NOx accumulation in end gas might induce super-knock in engines using EGR. A new normalized parameter ξ_a is introduced to quantify the regimes for different autoignition modes. Compared to the traditional counterpart parameter, ξ, used in previous studies, this new parameter is more suitable since it yields a detonation development regime in a C-shaped curve which is almost unaffected by the initial conditions. The relationship between ξ_a and ξ is also examined. With the increase of NO concentration gradient or temperature gradient, ξ_a always increases monotonously with ξ. Nevertheless, further investigation on the influence of initial condition on ξ_a-ξ relation is still needed.

Acknowledgments

This work is supported by National Natural Science Foundation of China (Nos. 51606091 and 91741126).

Supplementary materials

Supplementary material associated with this article can be found, in the online version, at doi:10.1016/j.proci.2018.06.063.

References

[1] Z. Wang, H. Liu, R.D. Reitz, *Prog. Energy Combust. Sci.* 61 (2017) 78–112.
[2] G. Kalghatgi, *Int. J. Engine Res.* 19 (2018) 7–20.
[3] T. Li, T. Yin, B. Wang, *Energy Convers. Manage.* 148 (2017) 1233–1247.
[4] Y. Putrasari, N. Jamsran, O. Lim, *Fuel* 200 (2017) 447–457.
[5] K. Cung, A.A. Moiz, X.C. Zhu, S.Y. Lee, *Proc. Combust. Inst.* 36 (2017) 3605–3612.
[6] H.A. El-Asrag, Y.G. Ju, *Combust. Flame* 161 (2014) 256–269.
[7] Y.B. Zeldovich, V.B. Librovich, G.M. Makhviladze, G.I. Sivashinsky, *Acta Astronaut.* 15 (1970) 313–321.
[8] Y.B. Zeldovich, *Combust. Flame* 39 (1980) 211–214.
[9] X.J. Gu, D.R. Emerson, D. Bradley, *Combust. Flame* 133 (2003) 63–74.
[10] D. Bradley, G.T. Kalghatgi, *Combust. Flame* 156 (2009) 2307–2318.
[11] G.T. Kalghatgi, D. Bradley, *Int. J. Engine Res.* 13 (2012) 399–414.
[12] L. Bates, D. Bradley, G. Paczko, N. Peters, *Combust. Flame* 166 (2016) 80–85.
[13] P. Dai, Z. Chen, S.Y. Chen, Y.G. Ju, *Proc. Combust. Inst.* 35 (2015) 3045–3052.
[14] P. Dai, Z. Chen, *Combust. Flame* 162 (2015) 4183–4193.
[15] P. Dai, C.K. Qi, Z. Chen, *Proc. Combust. Inst.* 36 (2017) 3643–3650.
[16] C.K. Qi, P. Dai, H. Yu, Z. Chen, *Proc. Combust. Inst.* 36 (2017) 3633–3641.
[17] T.H. Zhang, W.Q. Sun, Y.G. Ju, *Proc. Combust. Inst.* 36 (2017) 1539–1547.
[18] A. Dubreuil, F. Foucher, C. Mounaim-Rousselle, G. Dayma, P. Dagaut, *Proc. Combust. Inst.* 31 (2007) 2879–2886.
[19] J.B. Masurier, F. Foucher, G. Dayma, P. Dagaut, *Proc. Combust. Inst.* 35 (2015) 3125–3132.
[20] Z.Y. Chen, P. Zhang, Y. Yang, M.J. Brear, X. He, Z. Wang, *Combust. Flame* 186 (2017) 94–104.
[21] H.A. El-Asrag, Y.G. Ju, *Combust. Theory Model.* 17 (2013) 316–334.
[22] H. Zhao, L.N. Wu, C. Patrick, Z.H. Zhang, Y. Rezgui, X.L. Yang, G. Wysocki, Y.G. Ju, *Combust. Flame* (2018) Under review.
[23] U. Burke, K.P. Somers, P. O'Toole, et al., *Combust. Flame* 162 (2015) 315–330.
[24] Z.C. Shi, H.G. Zhang, H.T. Lu, H. Liu, A. Yunsheng, F.X. Meng, *Fuel* 194 (2017) 50–62.
[25] L. Pan, E.J. Hu, X. Meng, Z.H. Zhang, Z.H. Huang, *Int. J. Hydrogen Energy* 40 (2015) 5221–5235.
[26] W. Ye, J.C. Shi, R.T. Zhang, et al., *Energy Fuels* 30 (2016) 10900–10908.
[27] Z. Chen, M.P. Burke, Y.G. Ju, *Proc. Combust. Inst.* 32 (2009) 1253–1260.

Please cite this article as: P. Dai, Z. Chen, Effects of NOx addition on autoignition and detonation development in DME/air under engine-relevant conditions, Proceedings of the Combustion Institute (2018), https://doi.org/10.1016/j.proci.2018.06.063